



# Susceptibility assessment for rainfall-induced landslides using a revised logistic regression method

Xinfu Xing<sup>1</sup> · Chenglong Wu<sup>1</sup> · Jinhui Li<sup>1</sup> · Xueyou Li<sup>2</sup> · Limin Zhang<sup>3</sup> · Rongjie He<sup>1</sup>

Received: 19 July 2020 / Accepted: 25 November 2020 / Published online: 5 January 2021  
© Springer Nature B.V. 2021

## Abstract

Landslide susceptibility is the likelihood of a landslide occurring in an area. The logistic regression (LR) method is one of the most popular methods for landslide susceptibility assessment. For rainfall-induced landslides, yearly or monthly rainfall is commonly used to establish a landslide susceptibility model by the LR method. It is a static susceptibility model, which limits the application to predict future landslide probability under potential rainfall event. This study presents a revised logistic regression method to achieve dynamic landslide susceptibility prediction under cumulative daily rainfall. Five kinds of cumulative daily rainfall are used in the landslide susceptibility assessment. The latest landslide events are used to update the landslide susceptibility model. The receiver operation characteristic curve and area under curve are utilized to evaluate the prediction reliability. The landslide susceptibility assessment in Shenzhen is taken as an illustration of the proposed method. The result indicates the method is capable to achieve a high accuracy of 91.9% when the landslide susceptibility model is updated using seven extreme rainfall events in the past 10 years. This method provides an advance prediction of the potential geo-hazards for a large area using the future rainfall forecast.

**Keywords** Natural disaster · Landslide susceptibility · Rainfall-induced landslide · Logistic regression method

## 1 Introduction

Landslides, as one of the most common natural geologic hazards, could cause huge loss of lives and property. According to the geological hazard bulletins of China in the past 10 years, 90% of landslides were directly triggered by rainfall. For example, hundreds

---

✉ Jinhui Li  
jinhui.li@hit.edu.cn

<sup>1</sup> Department of Civil and Environmental Engineering, Harbin Institute of Technology (Shenzhen), Shenzhen University Town, Xili, Shenzhen 518055, China

<sup>2</sup> School of Civil Engineering, Sun Yat-Sen University, Guangzhou 510275, China

<sup>3</sup> Department of Civil and Environmental Engineering, The Hong Kong University of Science and Technology, Hong Kong, China

of landslides were triggered by the heavy rainfall event in Shenzhen on June 13–14, 2008. A severe rainfall event attacked Zhouqu, Gansu province on August 7, 2010, which caused a catastrophic accident with 1765 people died or missed (Li et al. 2010). Landslide susceptibility map portrays the landslides spatial distribution. It describes the relative likelihood of landslide occurrence based on the predisposing factors of a locale or site (Gupta and Joshi 1990; Guzzetti et al. 1999). Landslide susceptibility maps are used to study the landslides' spatial and temporal distribution, to analyze the slopes that are likely to fail, to develop mitigation measures. Landslide susceptibility assessment is regarded as an effective method for landslide prevention and mitigation in a large area.

Statistical methods are frequently used to analyze landslide susceptibility. The common statistical methods include logistic regression (LR) method (Koutsias and Kartaris 1998; Zhao et al. 2019), analytic hierarchy process (Wu and Chen 2009; Quan and Lee 2012), weight-of-evidence method (Lee et al. 2013; Riaz et al. 2018), support vector machines (Kavzoglu et al. 2014; Kumar et al. 2017) and artificial neural network method (Ermini et al. 2005; Bui et al. 2020; Liu et al. 2020; Zhang et al. 2020). The LR method has been one of the most popular methods to analyze landslide susceptibility because the calculated result is viewed as landslide probability by taking landslides and non-landslides as binary variables. However, the LR model is rarely used to predict landslide probability under future possible rainfall event when it is based on yearly or monthly rainfall which does not reflect the relationship between landslides and short-term cumulative rainfall. Hence, it is valuable to establish a reliable dynamic revised logistic regression (RLR) model for predicting future landslide probability.

The topographic and geological factors of slopes such as slope angle, elevation, lithology and aspect are important to assess the landslide susceptibility (Li et al. 2011; Li and Zhang 2011; Monsieurs et al. 2019; Zhu and Zhang 2019). The average annual rainfall or monthly rainfall is frequently used to establish the landslide susceptibility model (Chan et al. 2018). This model ignores the influence of short-term cumulative rainfall on landslide. The stability of slopes are highly depended on water content in soils that is affected by geological characteristics and a short-term cumulative rainfall event (Zhang et al. 2014; Li et al. 2015). Therefore, it is reasonable to study the short-term cumulative rainfall effect when establishing the susceptibility model for rainfall-induced landslides.

A LR model is established based on the landslide events by a specific proportion (Akgun 2012; Steger et al. 2017) or by their spatial distributions (Conoscenti et al. 2016). The LR model is not a proper model if the landslide susceptibility result is dissatisfying. It ignores the potential to improve the model's performance that is affected by the variations of landslides and predisposing factors. The landslide records are ponderable resources to revise the model. The landslide susceptibility model gets updated considering the new relation between landslide events and predisposing factors. By this way, it is possible to predict regional landslide probability precisely over a long-time span based on a RLR model.

The short-term cumulative rainfall effect and a dynamic reliable revision method are both indispensable to analyze or predict future landslide probability. This study focuses on the landslide susceptibility assessment based on a RLR method and its application to predict landslide probability by introducing short-term cumulative rainfall event. In Sect. 2, a brief introduction to the study area is presented. In Sect. 3, LR method, RLR method and validation method are introduced. The landslide susceptibility results are presented and discussed in Sects. 4 and 5 based on the data of study area and the methods above. The result shows that the proposed method has a better performance on landslide probability prediction, which is useful for further landslide evaluation, prevention and mitigation.

## 2 Study area and database analysis

### 2.1 study area

The study area is Shenzhen which is located in the south of China. It is bound by the longitudes of 113°45' E to 114°37' E and the latitude of 22°27' N to 22°52' N. The land area of Shenzhen is about 1997 km<sup>2</sup>. The location of the study area is illustrated in Fig. 1.

The climate of Shenzhen is a subtropical marine monsoon climate. The average annual rainfall ranges from 1700 to 2000 mm during 2008 to 2018. The rainfall occurring between May and September accounts for about 70% of the average annual rainfall. Shenzhen is characterized by hills that are scattered around the city. Landslides are easily triggered at special geological sites if the rainfall is heavy in a period.

One of the basic standards of landslide susceptibility assessment is “Past is the key to future.” It is worthy to analyze the relationship between landslides and the related factors (Zhang et al. 2011a, 2011b; Wang et al. 2019). In this study, landslide database, rainfall database and four geological databases (include slope angle, elevation, lithology and aspect) have been collected from the government departments, data archives and related scientific institute, respectively. The digital resources can be used directly during the landslide susceptibility assessment process. The paper records should be transformed into digital data prior to the application. The introduction to these databases is listed in Table 1.

### 2.2 Database source

#### 2.2.1 Landslide inventory

Rainfall-induced landslide events frequently occurred in Shenzhen. Four hundred eighty-six rainfall-induced landslide events were recorded from 2008 to 2018 according to the statistical standard of life or economic loss. Figure 2 depicts the locations and yearly

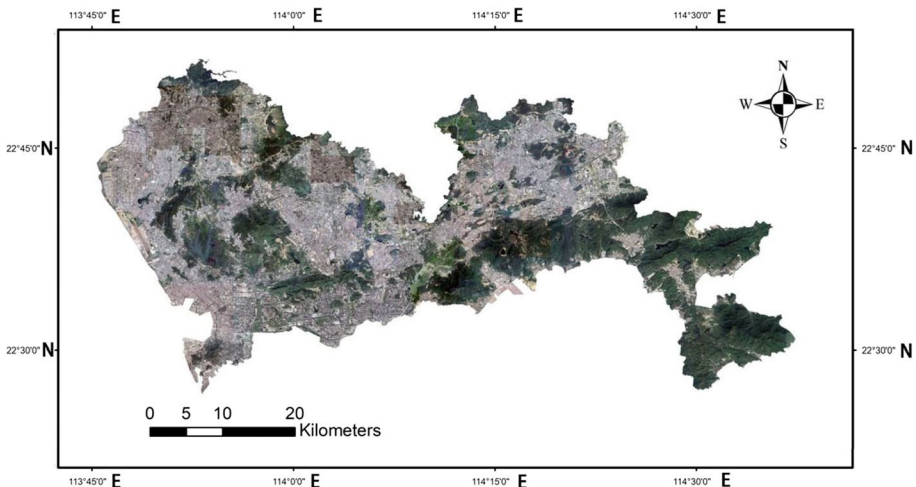
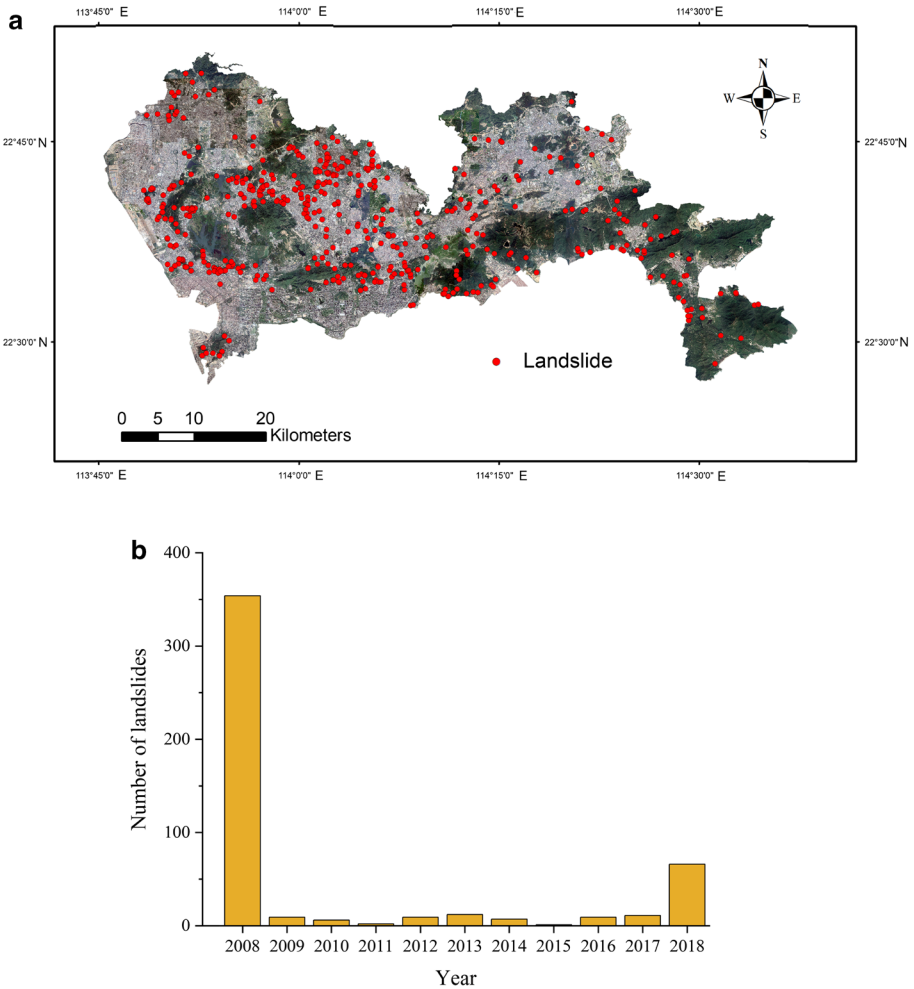


Fig. 1 Location of the study area

**Table 1** Databases used in the study

| Database  | Source                                                                                       |
|-----------|----------------------------------------------------------------------------------------------|
| Landslide | Planning and Natural Resources Bureau of Shenzhen Municipality                               |
| Rainfall  | Meteorological Bureau of Shenzhen Municipality                                               |
| Slope     | Geospatial Data Cloud Site, Computer Network Information Center, Chinese Academy of Sciences |
| Elevation |                                                                                              |
| Aspect    |                                                                                              |
| Lithology | National Geological Archives                                                                 |



**Fig. 2** Landslide locations (a) and distribution in each year (b) in Shenzhen from 2008 to 2018

distributions of the landslide events. Landslides spread all over Shenzhen as shown in Fig. 2a. Landslides mainly occurred around mountains. Some landslides scattered around the hills that are nestled in urban areas. Landslide events varied among years as shown in Fig. 2b. A large number of landslides occurred in 2008 and 2018, respectively. Three hundred fifty-four landslides occurred in 2008, which takes up 72.8% of those in the landslide inventory. Two hundred ninety-seven landslides occurred in June 2008. The number of the landslides for the four remarkable days (13 June, 14 June, 26 June and 27 June of 2008) is 188, 48, 32 and 29, respectively. A total of 66 landslides occurred in 2018, and 56% of the landslides take place on 30 August.

### 2.2.2 Rainfall database

Rainfall plays the predominant role in rainfall-induced landslides. The rainfall data from 2008 to 2018 is provided by Shenzhen Meteorological Bureau. The rainfall data are obtained from ten representative meteorological stations which scatter in the region of Shenzhen. The stations' location and typical daily rainfall records are listed in Table 2.

### 2.2.3 Geology database

Slope angle, elevation, lithology and aspect are utilized as typical geology factors. The factors should be processed before the establishment of the LR model. Lee et al. (2004) prove that the LR model has a poor performance when LR model works with a combination of continuous and categorical variables. In addition, the authors (Lee et al. 2004; Zhao et al. 2019) point out that the LR model using categorical variables showed excellent fit to training data. Considering that lithology and aspect are categorical variables rather than continuous variables, slope angle and elevation are also processed as categorical variables.

These factors are divided into different intervals among which the landslide events are classified. Hence, the criterion of the interval for slope angle and elevation are to balance the number of landslides in each interval. The classification of lithology and aspect is

**Table 2** Rainfall records of ten meteorological stations

| Station   | Location          | Daily rainfall (mm) |       |       |       |       |       |       |       |       |       |
|-----------|-------------------|---------------------|-------|-------|-------|-------|-------|-------|-------|-------|-------|
|           |                   | 08/06               | 09/06 | 10/06 | 11/06 | 12/06 | 13/06 | 14/06 | 15/06 | 16/06 | 17/06 |
| Zhuzilin  | (114°0', 22°32')  | 10.1                | 0     | 0     | 34.9  | 0.8   | 151   | 121.5 | 31.2  | 0     | 40.6  |
| Caiwuwei  | (114°6', 22°32')  | 7.7                 | 0     | 0.3   | 24    | 8.2   | 201.9 | 78.5  | 25.4  | 2     | 44.2  |
| Nanshan   | (113°55', 22°31') | 6.3                 | 0     | 0     | 60.6  | 0.5   | 95.9  | 114.7 | 32.9  | 1.3   | 16.4  |
| Yantian   | (114°15', 22°34') | 20.3                | 0     | 0.4   | 22.6  | 3.9   | 98.9  | 84.3  | 27    | 41.5  | 51.2  |
| Shiyan    | (113°53', 22°34') | 13.6                | 0     | 0     | 14.3  | 2.9   | 370.4 | 61.4  | 0.9   | 0.5   | 16    |
| Longgang  | (114°14', 22°43') | 5.9                 | 0     | 3.6   | 10.5  | 6.8   | 223.6 | 70.9  | 21.3  | 17.4  | 32.3  |
| Guangming | (113°57', 22°45') | 18.4                | 0     | 0     | 9     | 3.6   | 330.5 | 17.8  | 1.8   | 0     | 6.5   |
| Kengzi    | (114°21', 22°44') | 4.5                 | 0     | 0     | 7.9   | 16.5  | 283.5 | 50.4  | 14.6  | 15.4  | 68.8  |
| Xichong   | (114°31', 22°39') | 18.3                | 0     | 0     | 14.7  | 5.2   | 51.8  | 117.1 | 47.4  | 22.1  | 87.5  |
| Minzhi    | (114°1', 22°37')  | 5.2                 | 0     | 0     | 57.0  | 2.6   | 181.4 | 106.2 | 24.4  | 0.4   | 29.8  |

Daily rainfall data in 2008 is listed in the table. Date format is “DD-MM”

according to their natural characteristics. The classifications of the four geology factors are shown in Table 3.

**2.2.3.1 Slope angle** Slope angle is regarded as an important terrain feature that affects the stability of slopes. The larger slope angle of the hill is, the more likely to fail and slide. According to the database, the land area of slope angle that is below  $8^\circ$  accounts for 60% of the whole land area. The area of slope angle that ranges from  $8^\circ$  to  $15^\circ$ , and  $15^\circ$  to  $25^\circ$  accounts for 19% and 14% of the whole area, respectively. The distribution of slope angle is illustrated in Fig. 3a.

**2.2.3.2 Elevation** Elevation reflects the average landform of a region. The weather conditions are various in high-elevation areas. Hence, elevation is commonly regarded as an important factor for rainfall-induced landslides. Shenzhen is a coastal city where elevation ranges from the sea level (0 m) to 945 m. The average elevation is from 70 to 120 m. Shenzhen is characterized by a relatively high altitude in the southeast and a relatively low altitude in the central and the northwest. The elevation distribution of Shenzhen is shown in Fig. 3b.

**2.2.3.3 Lithology** Lithology directly determines the physical and mechanical properties of rocks and soils. Geological map records the lithology type of the strata. It is noted that the

**Table 3** The classes of four factors and its frequency ratio based on data of June 13–14, 2008

| Factor                    | Class                           | Number of landslide | A. Landslide ratio (%) | B. Class area ratio (%) | Frequency ratio (FR) (A/B) |
|---------------------------|---------------------------------|---------------------|------------------------|-------------------------|----------------------------|
| Slope angle               | $0^\circ$ – $8^\circ$           | 35                  | 14.83                  | 57.57                   | 0.26                       |
|                           | $8^\circ$ – $15^\circ$          | 63                  | 26.69                  | 18.92                   | 1.41                       |
|                           | $15^\circ$ – $25^\circ$         | 72                  | 30.50                  | 16.24                   | 1.88                       |
|                           | $> 25^\circ$                    | 66                  | 27.96                  | 7.27                    | 3.85                       |
| Elevation                 | 0–25 m                          | 20                  | 8.47                   | 25.12                   | 0.34                       |
|                           | 25–50 m                         | 41                  | 17.37                  | 22.94                   | 0.76                       |
|                           | 50–75 m                         | 78                  | 33.47                  | 17.74                   | 1.89                       |
|                           | $> 75$ m                        | 96                  | 40.68                  | 34.20                   | 1.19                       |
| Lithology                 | Alluvial                        | 17                  | 7.20                   | 5.17                    | 1.39                       |
|                           | Sandstone                       | 26                  | 11.02                  | 15.28                   | 0.72                       |
|                           | Coal-bearing clastic rock       | 5                   | 2.12                   | 1.91                    | 1.11                       |
|                           | Interbedded sandstone and shale | 47                  | 19.92                  | 19.42                   | 1.03                       |
|                           | Limestone                       | 27                  | 11.44                  | 15.62                   | 0.73                       |
| Aspect                    | Granite                         | 114                 | 48.31                  | 42.60                   | 1.13                       |
|                           | $0^\circ$ – $45^\circ$          | 32                  | 13.56                  | 14.28                   | 0.95                       |
|                           | $45^\circ$ – $90^\circ$         | 27                  | 11.44                  | 11.26                   | 1.02                       |
|                           | $90^\circ$ – $135^\circ$        | 35                  | 14.83                  | 12.20                   | 1.22                       |
|                           | $135^\circ$ – $180^\circ$       | 35                  | 14.83                  | 12.99                   | 1.14                       |
|                           | $180^\circ$ – $225^\circ$       | 36                  | 15.25                  | 13.65                   | 1.12                       |
|                           | $225^\circ$ – $270^\circ$       | 25                  | 10.59                  | 12.50                   | 0.85                       |
|                           | $270^\circ$ – $315^\circ$       | 24                  | 10.17                  | 12.10                   | 0.84                       |
| $315^\circ$ – $360^\circ$ | 22                              | 9.32                | 11.03                  | 0.85                    |                            |

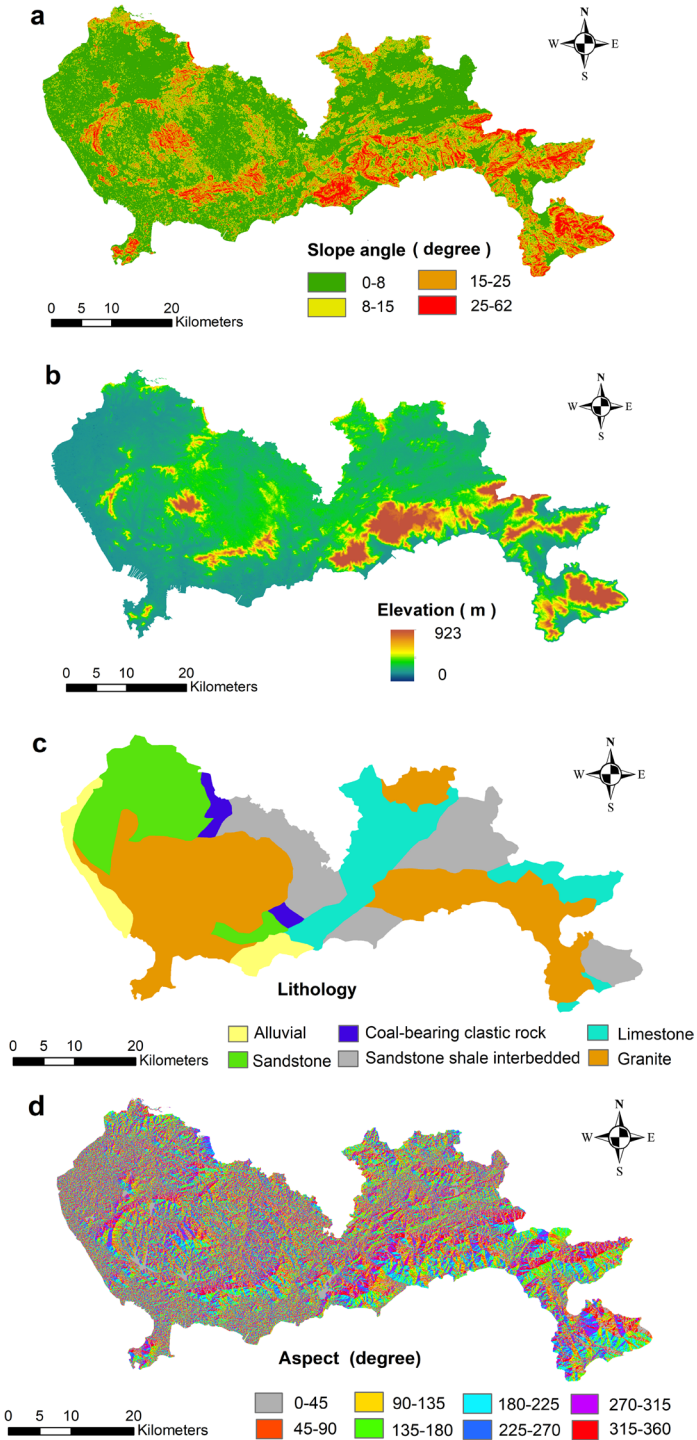


Fig. 3 Predisposing factors of Shenzhen: **a** slope angle, **b** elevation, **c** lithology and **d** aspect

weathered soil and residual materials in the surface of the landscape are also referred by the same lithology (e.g., granite rock and granite residual soils are referred as granite collectively). The digital lithological map is depicted based on the original paper lithological map (1: 200,000 scale). The lithological distribution is mapped in Fig. 3c. Granite is the most widespread lithological unit that covers 43% of the whole land area. It distributes at the high-elevation areas. The area of interbedded sandstone and shale is about 19% of the whole area. The area of sandstone is close to the area of limestone, which occupies about 15% and 16% of the whole area, respectively. The alluvial covers 5% of the whole area.

**2.2.3.4 Aspect** Aspect indicates the direction of a slope faces. The aspect of a slope is an important factor that affects water content in the slope soils because it affects the amount of sunlight striking the earth's surface (Li et al. 2011, 2014; Måren et al. 2015). Different aspects lead to a huge discrepancy of effective rainfall especially in high-elevation areas, which has great influences on landslide occurrence. Aspect is measured starting from the north as 0° and one clockwise cycle back to the north as 360°. Aspect was classified into the eight cardinal directions with an increment of 45° (N, NE, E, SE, S, SW, W, NW, N) and flat land (slope angle is 0°). The distribution of the aspect is shown in Fig. 3d.

### 2.3 Database analysis

The characteristics of landslides are extracted to analyze landslide susceptibility based on those databases above. The factors' characteristics were extracted by specific grids based on the GIS platform. In this study, the SRTM DEM (30 m) was utilized because it is an open free resource which has been used for decades in scientific research. The high-resolution DEM is not utilized because the performance of the landslide susceptibility model is not very sensitive to the spatial resolution from 5 to 30 m (Zhao et al. 2019). Besides, the high-resolution DEM (finer than 10 m) may decrease the representativeness of the local surface topography during the susceptibility assessment (Tarolli and Tarboton 2006). Therefore, it is reliable to extract the factors' characteristics from the SRTM DEM (30 m).

The predisposing factors are characterized into classes for further analysis. Rainfall in five cumulative periods is considered. The rainfall threshold of each class depends on the cumulative period. The first classes of the cumulative rainfall from 1-day to 5-day are 100, 120, 150, 180 and 200 mm, respectively. The increment each class is 50 mm for 1-day rainfall. The increment each class is 60 mm for 2-day to 5-day rainfall. Five cumulative rainfall maps were generated by the rainfall data of ten representative meteorological stations. Here, the kernel interpolation method was used to calculate the rainfall at various locations and generate the rainfall maps as it can effectively reduce the interpolation error by involving ridge parameters (Hoerl and Kennard 1970). The cumulative rainfall interpolations on June 13, 2008, are depicted in the examples in Fig. 4.

## 3 Method

### 3.1 LR method

The LR method is a predictive analysis process where the dependent variables are the events and the independent variables are formulated by the predisposing factors. The



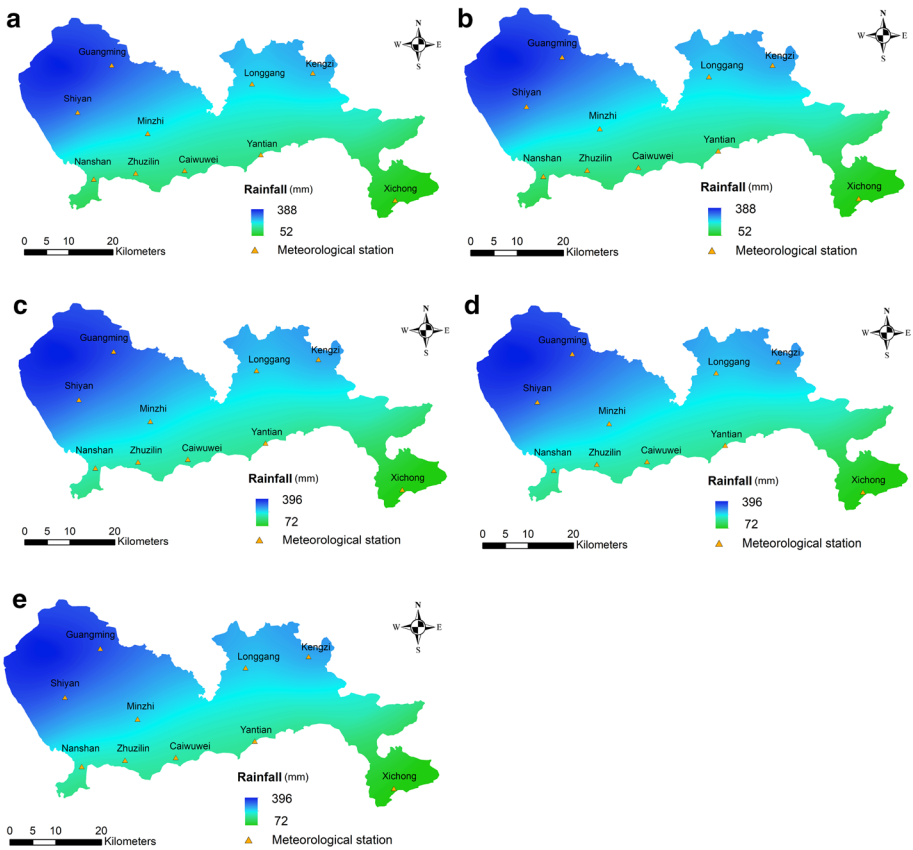


**Fig. 4** Interpolation map of cumulative rainfall of **a** 1-day, **b** 2-day, **c** 3-day, **d** 4-day and **e** 5-day before June 13, 2008.

dependent variables are dummy variables in the process of landslide susceptibility analysis. The value 0 refers to a non-landslide event (also called as negative cell) and 1 refers to a landslide event (positive cell).

When using the  $P(Y = 1) = \alpha + \beta x$  to calculate landslide probability, the outcome of the equation may be  $> 1$  or  $< 0$  mathematically, although the landslide probability must range from 0 to 1 from a practical point of view. To avoid this anomaly, the LR method forms the expression by creating the logit ( $P$ ) which is defined as:

$$\text{logit}(P) = \ln \frac{P(Y = 1)}{1 - P(Y = 1)} = \alpha + \beta_1 x_1 + \beta_2 x_2 + \dots + \beta_n x_n \quad (1)$$

where  $P(Y = 1)$  represents the predicted probability of landslide occurrence during the landslide susceptibility analysis,  $x_i$  ( $i = 1, 2, \dots, n$ ) represents the  $i$ th predisposing factor,  $\alpha$  and  $\beta_i$  ( $i = 1, 2, \dots, n$ ) are the coefficients of the predisposing factors. The process to calculate the coefficients refers to the previous literatures (King and Zeng 2001; Hosmer and Lemeshow 2005).

Equation (1) is transformed to Eq. (2):

$$P(Y = 1) = \frac{\exp(\alpha + \beta_1 x_1 + \beta_2 x_2 + \dots + \beta_n x_n)}{1 + \exp(\alpha + \beta_1 x_1 + \beta_2 x_2 + \dots + \beta_n x_n)} \quad (2)$$

Both landslide events (positive cells) and non-landslide events (negative cells) are important to establish the model. The landslide samples were set as positive cells in the original LR model after the preliminary analysis of landslides information. The non-landslides were set as negative cells and inputted into the LR model. By the Data Management Tools in ArcGIS, non-landslide points were selected randomly all over Shenzhen based on the criteria that non-landslide points were 200 m away from the landslide points and not located at the grids of water. Meanwhile, ten subsets of non-landslides are created to calculate the average value for evaluating the model's performance considering the randomness of the non-landslide samples.

### 3.2 RLR method

The LR model has a unique expression when it is established. Landslide susceptibility index (LSI) is frequently used to assess the relation between landslide events and predisposing factors in the established landslide susceptibility model (Devkota et al. 2013; Kavoura and Sabatakakis 2020). The  $LSI_{ij}$  of the class  $j$  of the factor  $i$  is shown as follows:

$$LSI_{ij} = W_i \times FR_{ij} \quad (3)$$

where  $W_i$  is the weight of the factor  $i$ ,  $FR_{ij}$  is the frequency ratio (FR) of the class  $j$  of the factor  $i$ .

The weight of the factors (e.g., rainfall, slope angle, elevation, lithology and aspect)  $W_i$  can be evaluated by the area under curve (AUC) value using the method proposed by Kavoura and Sabatakakis (2020). The curve refers to the receiver operation characteristic (ROC) curve. Different scenarios are used to obtain each factor's weight. The scenario-1 consists of all five factors (rainfall, slope angle, elevation, lithology and aspect). From scenario-2 to scenario-6, one of five factors is excluded in sequence to evaluate the weight of this excluded factor separately. If the AUC value is high, the weight of the excluded factor is small and vice versa. Note that five cumulative periods of rainfall are discussed in each scenario. The method to assess the relative weight by AUC is introduced simply as below:

$$W_i = \frac{1 - AUC_{ave}}{\sum (1 - AUC_{ave})} \quad (4)$$

where  $(1 - AUC_{ave})$  refers to the credibility of the excluded factor.

$$FR_{ij} = \frac{L_{ij}}{A_{ij}} \quad (5)$$

where  $L_{ij}$  is the landslide ratio of the class  $j$  of the factor  $i$ ,  $A_{ij}$  is the area ratio of the class  $j$  of the factor  $i$ .  $FR_{ij}$  varies as more data are added in the LR model. It is noted that the distribution of every rainfall varies widely. This study assumes that the rainfall's weight varies, and  $FR_{ij}$  value keeps the same in order to avoid statistical anomaly caused by extreme rainfall events (e.g., rainfall concentrated in small regions or the quick movement of rainfall center).

The weight of each factor and the FR of each class of factor change when new landslide events are added into the previous landslide susceptibility model, which results in the

variation of the LSI dependently. The  $\Delta LSI_{ij}^{(k)}$  which denotes the LSI variation of the class  $j$  of the factor  $i$  after the  $k$ th time of adding landslide events is obtained as follows:

$$\Delta LSI_{ij}^{(k)} = LSI_{ij}^{(k)} - LSI_{ij}^{(k-1)} \tag{6}$$

where  $LSI_{ij}^{(k)}$  is the LSI of the class  $j$  of the factor  $i$  after the  $k$ th time of adding landslide events ( $k = 1, 2, \dots, m$ ).

For the local grid  $g$  to be predicted, the corresponding total LSI variation  $\Delta LSI_{ij}^{g(k)}$  can be obtained as follows:

$$\begin{aligned} \Delta LSI_{ij}^{g(k)} &= \sum_{i=1}^n \Delta LSI_{ij_g}^{(k)} \\ &= \sum_{i=1}^n \left[ LSI_{ij_g}^{(k)} - LSI_{ij_g}^{(k-1)} \right] \end{aligned} \tag{7}$$

where  $\Delta LSI_{ij_g}^{(k)}$  and  $LSI_{ij_g}^{(k)}$  are the LSI variation and the LSI of the class  $j_g$  of the factor  $i$  corresponding to the grid  $g$  after the  $k$ th time of adding landslide events, respectively.  $LSI_{ij_g}^{(k-1)}$  is the LSI of the class  $j_g$  of the factor  $i$  corresponding to the grid  $g$  after the  $(k-1)$ th time of adding landslide events.

The coefficients change when new landslide events are added into the LR model. Then, Eq. (2) can be transformed to:

$$P^{g(k)}(Y = 1) = \frac{\exp [\alpha + \beta_1 x_1 + \beta_2 x_2 + \dots + \beta_n x_n + \Delta LSI^{g(k)}]}{1 + \exp [\alpha + \beta_1 x_1 + \beta_2 x_2 + \dots + \beta_n x_n + \Delta LSI^{g(k)}]} \tag{8}$$

where  $P^{g(k)}(Y = 1)$  is the landslide probability for the local grid  $g$  to be predicted after the  $k$ th time of adding landslide events.

The process of event-added is regarded as a dynamic revision process by this way. As a consequence, the LR model is revised when landslide events and related factors are added. It is helpful to predict landslide probability in the future rainfall event.

### 3.3 Validation method

Landslide database records the landslide events occurred from 2008 to 2018. There were 188 landslides on 13 June and 38 landslides on 14 June of 2008, respectively. Two hundred twenty-six landslides were set as positive cells in the traditional LR model at first. King and Zeng (2001) proved that the LR model shows the best estimate to training samples when the non-landslide and landslide samples are applied equally if a limited landslide inventory is available. Therefore, it is the same amount of non-landslide samples as the landslide samples are applied in this study. Five factors were studied in the original LR model. Note that rainfall refers to five periods of cumulative rainfall (1-day to 5-day).

During the process of validation, the landslide samples were randomly divided into a training group (70% of the samples) and a validation group (30% of the samples). The non-landslide samples are divided by the same way.

The ROC curve and AUC are used to assess the performance of the LR model. The ROC curve is constructed by plotting sensitivity (true positive rate, TPR) against specificity (false positive rate, FPR). The TPR is the proportion of cells that are correctly predicted to be positive in positive cells. The FPR is the proportion of cells that are incorrectly

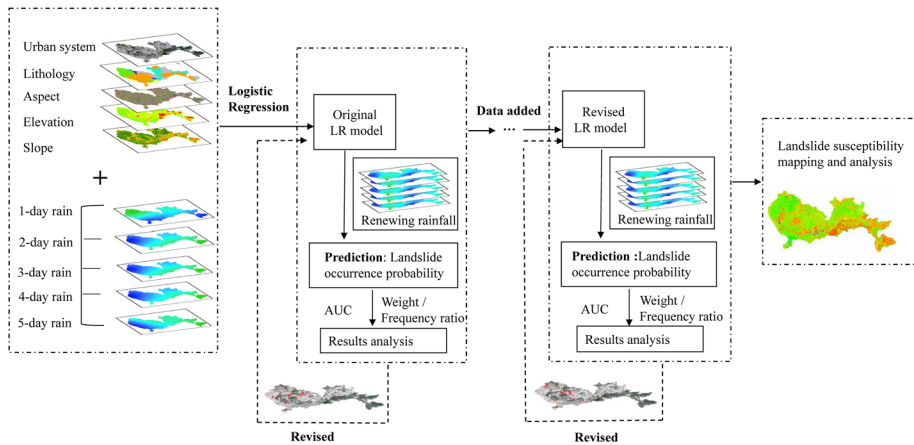


**Fig. 5** Simplified flowchart of research methodology

**Table 4** Success rate of validation samples of the original LR model

| Category | Success rate of ten subsets (%) |      |      |      |      |      |      |      |      |      | Ave  |      |
|----------|---------------------------------|------|------|------|------|------|------|------|------|------|------|------|
|          | 1                               | 2    | 3    | 4    | 5    | 6    | 7    | 8    | 9    | 10   |      |      |
| 1-D      | N-L                             | 68.0 | 73.3 | 78.7 | 73.3 | 81.3 | 74.7 | 72.0 | 76.0 | 74.7 | 72.0 | 74.4 |
|          | L                               | 73.0 | 77.8 | 69.8 | 77.8 | 69.8 | 74.6 | 76.2 | 69.8 | 68.3 | 74.6 | 73.2 |
| 2-D      | N-L                             | 76.0 | 73.3 | 80.0 | 76.0 | 76.0 | 72.0 | 77.3 | 76.0 | 69.3 | 72.0 | 74.8 |
|          | L                               | 77.8 | 72.4 | 76.2 | 77.8 | 71.4 | 76.2 | 76.2 | 69.8 | 74.6 | 76.3 | 74.9 |
| 3-D      | N-L                             | 75.5 | 73.3 | 72.0 | 73.3 | 73.6 | 76.0 | 76.0 | 76.0 | 72.0 | 80.0 | 75.2 |
|          | L                               | 76.2 | 77.8 | 74.6 | 76.2 | 72.3 | 76.2 | 76.2 | 73.0 | 76.2 | 76.2 | 75.5 |
| 4-D      | N-L                             | 73.3 | 74.7 | 76.0 | 77.3 | 73.0 | 76.0 | 77.3 | 80.0 | 73.3 | 78.7 | 76.0 |
|          | L                               | 73.0 | 77.8 | 74.6 | 76.2 | 75.8 | 77.8 | 77.8 | 75.8 | 74.2 | 74.2 | 75.7 |
| 5-D      | N-L                             | 75.2 | 76.0 | 77.3 | 76.3 | 74.7 | 73.3 | 72.3 | 74.7 | 73.3 | 73.3 | 74.6 |
|          | L                               | 76.2 | 74.6 | 73.0 | 73.0 | 71.4 | 74.6 | 74.6 | 68.3 | 71.4 | 69.8 | 72.7 |

X-D refers to model based on x-day rainfall. N-L refers to non-landslide prediction. L refers to landslide prediction

predicted to be positive out of all negative observations. The performance of the LR model is regarded as acceptable, excellent and outstanding performance when the AUC is larger than 0.7, 0.8 and 0.9, respectively.

The simplified flowchart in this study is illustrated in Fig. 5.

## 4 Results

### 4.1 Performance of LR model

Table 4 lists the success rate of the validation samples. The cumulative rainfall affects the success rate of the LR model. The success rate of landslides is not the same as the success

rate of non-landslides in the same cumulative rainfall condition. The average success rate under 4-day cumulative rainfall is the highest where the average success rate is 76.0% for non-landslides validation and 75.7% for landslides validation. The average success rate under 5-day cumulative rainfall is the worst where the success rate is 74.6% for non-landslides and 72.7% for landslides validation.

Figure 6 depicts the distribution of the ROC curves and the AUC values. All combinations show excellent fittings to their training data because the mean value of AUC is over 0.8. Among five categories of cumulative rainfall, the mean AUC value of 4-day model is the highest (0.857) and the AUC of 3-day ranks the second (0.855). The mean AUC value of 1-day model is the lowest (0.842).

The model of 4-day rainfall has the highest success rate and AUC, which indicates it behaves the best performance. Therefore, the model of 4-day rainfall is utilized to predict landslide probability in next steps.

## 4.2 Prediction by LR model

The outcome calculated by Eq. (2) represents the landslide probability (Bhandary et al. 2013; Devkota et al. 2013). By introducing 4-day cumulative rainfall of June 23–26, 2008, into the model, the predictive landslide occurrence probability on 26 June was analyzed. Thirty-two landslide events were recorded on that day. The prediction to a landslide site is regarded as a successful prediction when the predictive landslide probability on site is over 0.5 (Devkota et al. 2013; Jiang et al. 2013).

The first predictions by the LR model are not satisfying. Eighteen landslide events were predicted with a landslide probability over 0.5, which accounts for 56.3% (18/32) of the recorded landslide events. Fourteen landslide events are judged as non-landslides because the predictive probability is below 0.5. The original LR model is revised according to the variation of the LSI when new landslide events are added.

## 4.3 Weight and FR value

Table 5 lists the weight of each factor in the original LR model. The weight differs from factor to factor. The weight of slope angle, rainfall, elevation, lithology and aspect decreases in order. The weight of slope angle is 0.242, which indicates the slope angle is the highest-weight factor in the original LR model. The weight of rainfall is 0.241 that

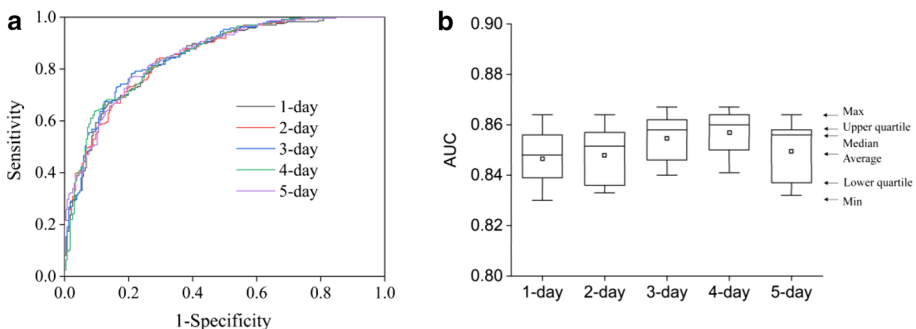


**Fig. 6** Performance of model based on five cumulative rainfall, **a** ROC curves and **b** AUC value

**Table 5** Weight of each factor in the original LR model of 4-day rainfall

| Scenario | Factor checked | AUC <sub>ave</sub> | 1–AUC <sub>ave</sub> | Weight (1–AUC <sub>ave</sub> )/Summary |
|----------|----------------|--------------------|----------------------|----------------------------------------|
| 2        | Rainfall       | 0.776              | 0.224                | 0.241                                  |
| 3        | Slope angle    | 0.775              | 0.225                | 0.242                                  |
| 4        | Elevation      | 0.835              | 0.165                | 0.178                                  |
| 5        | Lithology      | 0.838              | 0.162                | 0.175                                  |
| 6        | Aspect         | 0.847              | 0.153                | 0.165                                  |
|          | Summary        |                    | 0.929                | 1                                      |

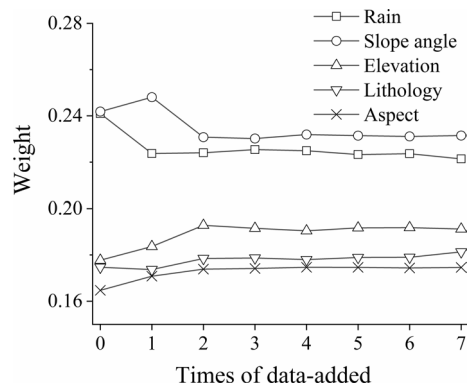
is close to the weight to slope angle. The weight of elevation and lithology is 0.178 and 0.175, respectively. Aspect is the least-weight factor, and its weight is 0.165. Slope angle and rainfall are most important predisposing factors in the original LR model.

When new landslide events are added into the LR model, the new weights of each factor are discussed. Figure 7 shows the varied weights during the event-added process. The weight of slope angle increases from 0.242 to 0.248 in the beginning and decreases to 0.231. Then it keeps steady with the value of 0.231 from third time to the end. The rainfall’s weight decreases from 0.241 to 0.224 in the first two times and varies softly in the later revisions. The variation mode of elevation, lithology and aspect differs from slope angle and rainfall. Their weights have small growths at first two times and remain constant in the later times. Five factors’ weights begin to be steady gradually, which indicates that factors in the susceptibility model keep stable when landslide samples cover enough predisposing conditions.

The FR of five factors performs different variations during the event-added process. Figure 8 illustrates the FR of each factor. The FR in the slope angle of 0° to 8° varies little when landslide events are added, and the FR of elevation under 25 m varies little as the same, which indicates landslides rarely took place in these two classes. The landslides are more inclined to take place in other classes of slope angle and elevation. The FR value of slope angle and elevation in other classes keeps rising slowly. It is a complicated variation in FR of lithology and aspect; the FR value increases randomly as the events are added.

Figure 9 shows the LSI results calculated as Eq. (3) when landslide events are added into the original LR model. The LSI of each factor varies during the dynamic process. New

**Fig. 7** The weights of five factors during the event-added process based on model of 4-day rainfall.



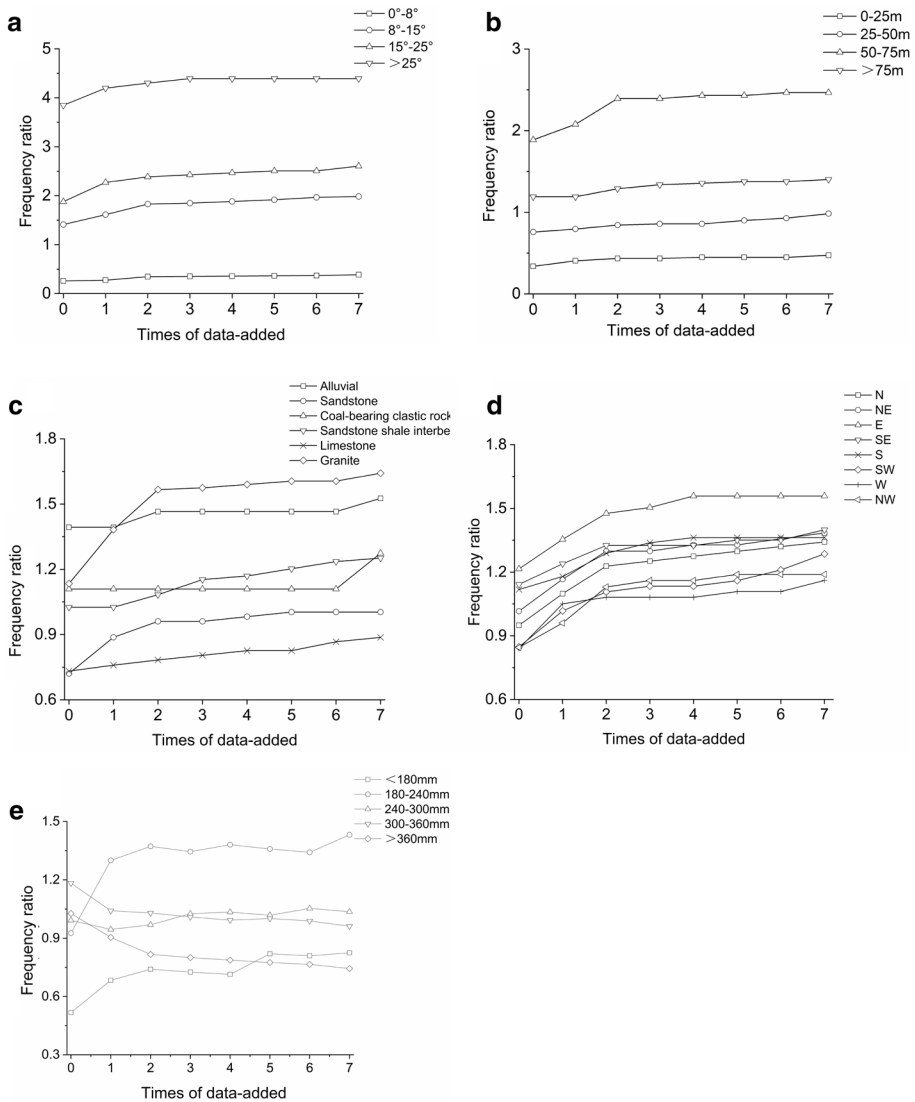


**Fig. 8** The frequency ratio of each class of **a** slope angle, **b** elevation, **c** lithology, **d** aspect and **e** 4-day rainfall

LSI of the LR model is more representative than the previous model. In this dynamic process, the statistical anomaly of the model decreases, which helps to get a reliable relation between the model and factors.

### 4.4 Performance of RLR model

Figure 10 shows the landslide prediction outcome based on the original LR model and RLR model. The accuracy of the RLR model is higher than that of the original LR model,

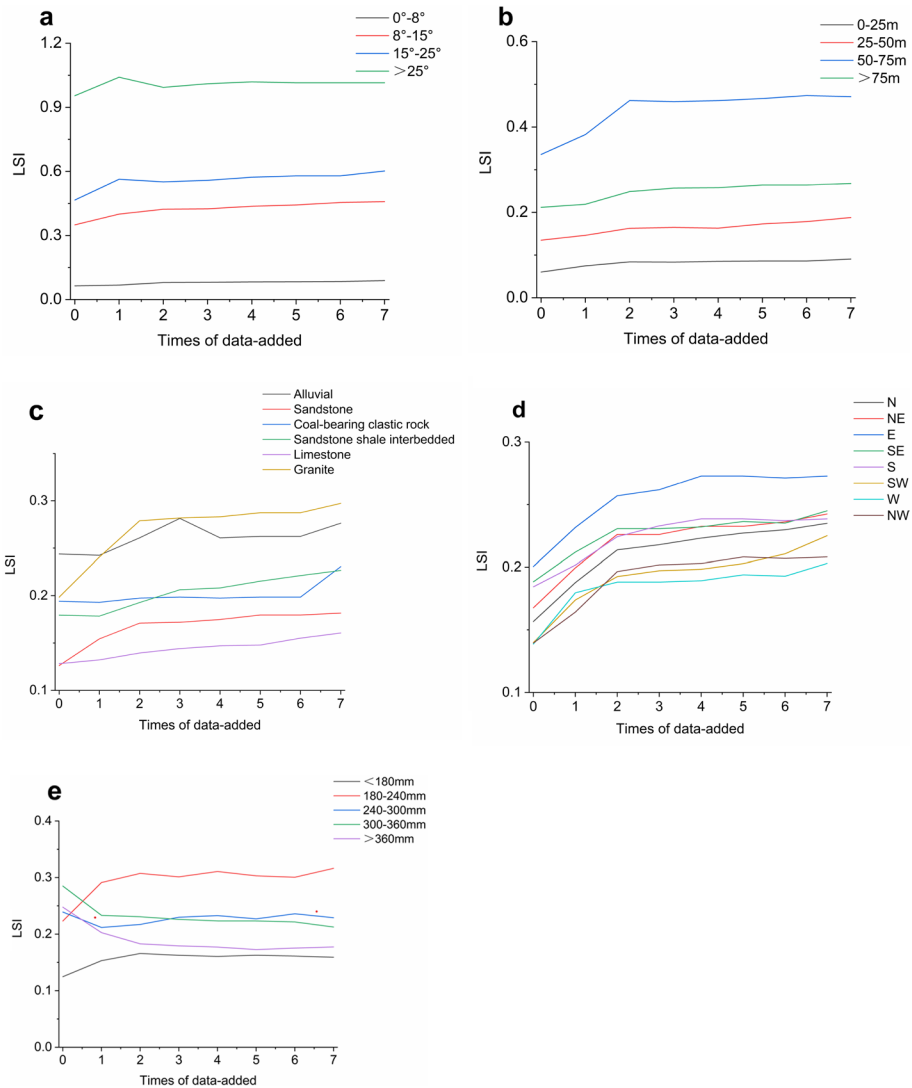


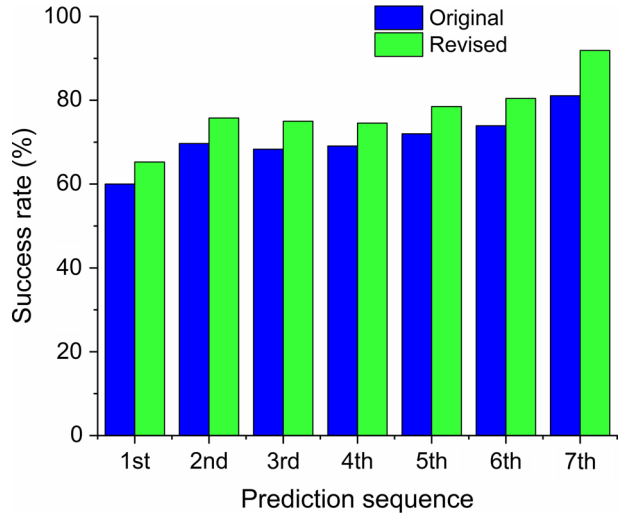
**Fig. 9** The landslide susceptibility index (LSI) during event-added process of **a** slope angle, **b** elevation, **c** lithology, **d** aspect and **e** 4-day rainfall

which indicates the RLR method works. The prediction accuracy rises from 65.3% to 91.9% as revision times increase. In the last prediction, the models were aimed to predict regional landslide probability on August 30, 2018, when 37 rainfall-triggered landslide events were recorded. The prediction accuracy reaches to 81.1% (30/37) of 4-day rainfall by the LR model. It rises to 91.9% (34/37) by the RLR model. The RLR model has an obvious improvement in future landslide probability prediction by introducing rainfall events compared with the original LR model.

Three landslide events were predicted as non-landslides by the RLR model of 4-day rainfall. They located at the hills which are closed to the roadway in the urban areas,



**Fig. 10** Landslide prediction accuracy based on original (LR) and revised (RLR) model of the cumulative rainfall of 4-day



where inner geological structures of the hills may have been highly influenced by human activities in the past few years. According to the calculation of the RLR model on 4-day rainfall, the landslide susceptibility distribution in Shenzhen is illustrated in Fig. 11. The locations of realistic landslide events are highly consistent with the regions where landslide susceptibility value is over 0.5.

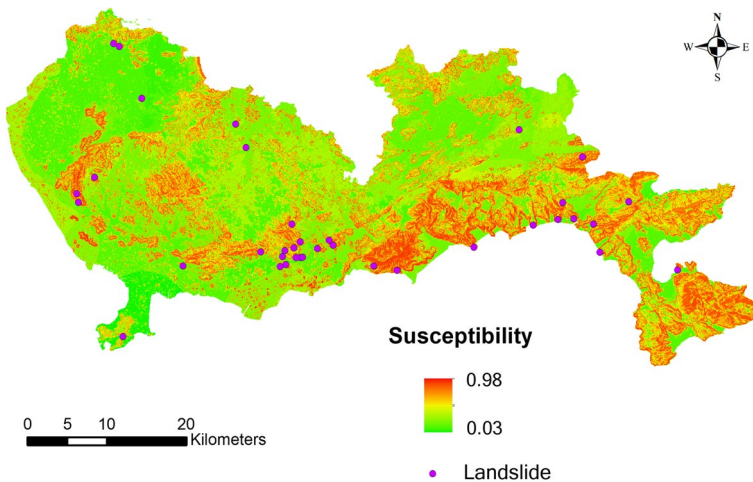


**Fig. 11** Landslide susceptibility map (4-day rainfall) and the locations of recorded landslide events on August 30, 2018

## 5 Discussions

### 5.1 Influence of cumulative rainfall effect

The model of 4-day cumulative rainfall yields the highest AUC value among the original LR models from 1-day to 5-day cumulative rainfall. The AUC of the 3-day rainfall model is the second highest. There are two main reasons that can be explained to this trend. First, short-term cumulative rainfall will lead to a huge discrepancy in water content of the soils, which significantly affects the slope stability (Li et al. 2017; Song et al. 2017, 2018). Second, the rainfall interval between two rainfall events commonly extends to days or weeks in Shenzhen from the weather records, which indicates that short-term cumulative rainfall is more representative to take susceptibility assessment for rainfall-induced landslides. The result in this study also agrees that the period of useful antecedent rainfall for landslide prediction should not exceed a week (Ma et al. 2014; Monsieurs et al. 2019).

### 5.2 Performance of LR model in event-added process

The proposed method takes the variation of weight and FR of factors into consideration. The LR model is revised by the LSI variation when more landslide events are added. The weight and FR vary during the revision process. Consider that the changes are helpful to revise the random statistic dispersion caused by some extreme landslide events. For instance, the weight of each factor increases except rainfall during the first time of event added. The recorded landslide events were occurred on June 25–26, 2008, when typhoon Fengshen swept Shenzhen with a speed over 30 m/s. A moderate future rainfall event easily triggers slopes to slide because some natural slopes were probably destabilized by plant-uprooting during the extreme typhoon event.

### 5.3 Prediction accuracy of RLR model

The original LR model predicts poorly in landslide probability. The prediction accuracy of the original LR model is less than 60%. However, the RLR model achieves the update that helps to predict landslide probability better. The RLR model gets a more satisfying prediction with an accuracy of 91.9% that is higher than the accuracy of the LR model. Besides, the proposed method shows a satisfying prediction accuracy compared with previous studies on landslide susceptibility by the LR method or neighboring areas (Table 6). Therefore,

**Table 6** Comparison of landslide prediction accuracies by LR method

| Author (year)          | Study area         | Numbers of factors | Prediction accuracy (%) |
|------------------------|--------------------|--------------------|-------------------------|
| Dai and Lee (2003)     | Hong Kong, China   | 7                  | 89.5                    |
| Bhandary et al. (2013) | Shikoku, Japan     | 8                  | Below 65.0              |
| Jiang et al. (2013)    | Shenzhen, China    | 1                  | 79.8                    |
| Ramani et al. (2011)   | Kodaikkanal, India | 10                 | 85.3                    |
| Lee et al. (2013)      | Gangwo, Korea      | 15                 | 85.4                    |
| This paper             | Shenzhen, China    | 5                  | 91.9                    |

it can be stated that the results achieved in this study are meaningful to landslide prediction and prevention.

## 6 Conclusions

This study demonstrates that the RLR model can be successfully used to predict landslide probability by introducing cumulative rainfall. Some remarkable conclusions can be drawn:

- (1) It is possible to establish a LR model to predict landslide probability based on short-term cumulative rainfall. The performance of the LR model varies with cumulative rainfall periods. The LR model of 4-day rainfall shows best reliability in the study area.
- (2) It is significant to update the LR model when the landslide events are added into the model. The RLR model gets revised according to the changes of weight and FR. The RLR model performs better than the original model to predict landslide probability. The new RLR model is optimal to get advance predictions on future landslide probability, which is helpful to regional landslide prevention and mitigation.

**Acknowledgements** This work was supported by Shenzhen Science and Technology Research & Development Fund (JCYJ20180507183854827), National Natural Science Foundation of China (No. 51909288) and the Guangdong Provincial Department of Science and Technology (2019ZT08G090). We are grateful to Planning and Natural Bureau and Meteorological Bureau of Shenzhen Municipality for providing landslide and rainfall data, respectively, in this study. Great thanks to Dr. Qianzhu Zhang and Ms. Jianmei Yan of Changjiang River Scientific Research Institute (CRSRI) for the help with the GIS software operation.

## Compliance with ethical standards

**Conflict of interest** The authors declare that they have no known competing financial interests or personal relationships that could have appeared to influence the work reported in this paper.

## References

- Akgun A (2012) A comparison of landslide susceptibility maps produced by logistic regression, multi-criteria decision, and likelihood ratio methods: a case study at İzmir, Turkey. *Landslides* 9:93–106. <https://doi.org/10.1007/s10346-011-0283-7>
- Bhandary NP, Dahal RK, Timilsina M, Yatabe R (2013) Rainfall event-based landslide susceptibility zonation mapping. *Nat Hazards* 69:365–388. <https://doi.org/10.1007/s11069-013-0715-x>
- Bui DT, Tsangaratos P, Nguyen V-T, van Liem N, Trinh PT (2020) Comparing the prediction performance of a deep learning neural network model with conventional machine learning models in landslide susceptibility assessment. *Catena* 188:104426. <https://doi.org/10.1016/j.catena.2019.104426>
- Chan H-C, Chen P-A, Lee J-T (2018) Rainfall-induced landslide susceptibility using a rainfall-runoff model and logistic regression. *Water* 10:1354. <https://doi.org/10.3390/w10101354>
- Conoscenti C, Rotigliano E, Cama M, Caraballo-Arias NA, Lombardo L, Agnesi V (2016) Exploring the effect of absence selection on landslide susceptibility models: a case study in Sicily, Italy. *Geomorphology* 261:222–235. <https://doi.org/10.1016/j.geomorph.2016.03.006>
- Dai FC, Lee CF (2003) A spatiotemporal probabilistic modelling of storm-induced shallow landsliding using aerial photographs and logistic regression. *Earth Surf Proc Land* 28(5):527–545. <https://doi.org/10.1002/esp.456>
- Devkota KC, Regmi AD, Pourghasemi HR, Yoshida K, Pradhan B, Ryu IC, Dhital MR, Althuwaynee OF (2013) Landslide susceptibility mapping using certainty factor, index of entropy and logistic regression

- models in GIS and their comparison at Mugling-Narayanghat road section in Nepal Himalaya. *Nat Hazards* 65:135–165. <https://doi.org/10.1007/s11069-012-0347-6>
- Ermini L, Catani F, Casagli N (2005) Artificial neural networks applied to landslide susceptibility assessment. *Geomorphology* 66:327–343. <https://doi.org/10.1016/j.geomorph.2004.09.025>
- Gupta RP, Joshi BC (1990) Landslide hazard zoning using the GIS approach—A case study from the Ramganga catchment, Himalayas. *Eng Geol* 28:119–131
- Guzzetti F, Carrara A, Cardinali M, Reichenbach P (1999) Landslide hazard evaluation: a review of current techniques and their application in a multi-scale study, Central Italy. *Geomorphology* 31:181–216
- Hoerl AE, Kennard RW (1970) Ridge regression: biased estimation for nonorthogonal problems. *Technometrics* 12:55–67. <https://doi.org/10.1080/00401706.1970.10488634>
- Hosmer DW, Lemeshow S (2005) *Applied logistic regression*, 2nd edn. Wiley, Hoboken, pp 1–46. <https://doi.org/10.1002/0471722146.ch2>
- Jiang G, Tian Y, Xiao C (2013) GIS-based rainfall-triggered landslide warning and forecasting model of Shenzhen. 21st international conference on geoinformatics conference on geoinformatics, pp 1–5. <https://doi.org/https://doi.org/10.1109/GeoInformatics.2013.6626026>
- Kavoura K, Sabatakakis N (2020) Investigating landslide susceptibility procedures in Greece. *Landslides* 17:127–145. <https://doi.org/10.1007/s10346-019-01271-y>
- Kavzoglu T, Sahin EK, Colkesen I (2014) Landslide susceptibility mapping using GIS-based multi-criteria decision analysis, support vector machines, and logistic regression. *Landslides* 11:425–439. <https://doi.org/10.1007/s10346-013-0391-7>
- King G, Zeng L (2001) Logistic regression in rare events data. *Polit Anal* 9(2):137–163. <https://doi.org/10.1093/oxfordjournals.pan.a004868>
- Koutsias N, Karteris M (1998) Logistic regression modelling of multitemporal thematic mapper data for burned area mapping. *Int J Remote Sens* 19:3499–3514. <https://doi.org/10.1080/014311698213777>
- Kumar D, Thakur M, Dubey CS, Shukla DP (2017) Landslide susceptibility mapping and prediction using Support Vector Machine for Mandakini River Basin, Garhwal Himalaya, India. *Geomorphology* 295:115–125. <https://doi.org/10.1016/j.geomorph.2017.06.013>
- Lee S, Ryu J-H, Won J-S, Park H-J (2004) Determination and application of the weights for landslide susceptibility mapping using an artificial neural network. *Eng Geol* 71:289–302. [https://doi.org/10.1016/S0013-7952\(03\)00142-X](https://doi.org/10.1016/S0013-7952(03)00142-X)
- Lee S, Hwang J, Park I (2013) Application of data-driven evidential belief functions to landslide susceptibility mapping in Jinbu, Korea. *Catena* 100:15–30. <https://doi.org/10.1016/j.catena.2012.07.014>
- Li JH, Zhang LM (2011) Study of desiccation crack initiation and development at ground surface. *Eng Geol* 123:347–358. <https://doi.org/10.1016/j.enggeo.2011.09.015>
- Li C, Ma T, Zhu X (2010) aiNet- and GIS-based regional prediction system for the spatial and temporal probability of rainfall-triggered landslides. *Nat Hazards* 52:57–78. <https://doi.org/10.1007/s11069-009-9351-x>
- Li JH, Zhang LM, Li X (2011) Soil-water characteristic curve and permeability function for unsaturated cracked soil. *Can Geotech J* 48:1010–1031. <https://doi.org/10.1139/t11-027>
- Li X, Zhang L-M, Wu L-Z (2014) A framework for unifying soil fabric, suction, void ratio, and water content during the dehydration process. *Soil Sci Soc of Am J* 78:387–399. <https://doi.org/10.2136/sssaj2013.08.0362>
- Li D-Q, Jiang S-H, Cao Z-J, Zhou W, Zhou C-B, Zhang L-M (2015) A multiple response-surface method for slope reliability analysis considering spatial variability of soil properties. *Eng Geol* 187:60–72. <https://doi.org/10.1016/j.enggeo.2014.12.003>
- Li JH, Lu Z, Guo LB, Zhang LM (2017) Experimental study on soil-water characteristic curve for silty clay with desiccation cracks. *Eng Geol* 218:70–76. <https://doi.org/10.1016/j.enggeo.2017.01.004>
- Liu Z-q, Guo D, Lacasse S, Li J-h, Yang B-b, Choi J-c (2020) Algorithms for intelligent prediction of landslide displacements. *J Zhejiang Univ Sci A* 21:412–429. <https://doi.org/10.1631/jzus.A2000005>
- Ma T, Li C, Lu Z, Wang B (2014) An effective antecedent precipitation model derived from the power-law relationship between landslide occurrence and rainfall level. *Geomorphology* 216:187–192. <https://doi.org/10.1016/j.geomorph.2014.03.033>
- Måren IE, Karki S, Prajapati C, Yadav RK, Shrestha BB (2015) Facing north or south: Does slope aspect impact forest stand characteristics and soil properties in a semiarid trans-Himalayan valley? *J Arid Environ* 121:112–123. <https://doi.org/10.1016/j.jaridenv.2015.06.004>
- Monsieurs E, Dewitte O, Demoulin A (2019) A susceptibility-based rainfall threshold approach for landslide occurrence. *Nat Hazards Earth Sys Sci* 19:775–789. <https://doi.org/10.5194/nhess-19-775-2019>
- Quan H-C, Lee B-G (2012) GIS-based landslide susceptibility mapping using analytic hierarchy process and artificial neural network in Jeju (Korea). *KSCE J Civ Eng* 16:1258–1266. <https://doi.org/10.1007/s12205-012-1242-0>

- Ramani SE, Pitchaimani K, Gnanamanickam VR (2011) GIS based landslide susceptibility mapping of Tevankarai Ar sub-watershed, Kodaikkanal, India using binary logistic regression analysis. *J MT Sci* 8(4):505–517. <https://doi.org/10.1007/s11629-011-2157-9>
- Riaz MT, Basharat M, Hameed N, Shafique M, Luo J (2018) A data-driven approach to landslide-susceptibility mapping in mountainous terrain: case study from the Northwest Himalayas. *Pak Nat Hazards Rev* 19:5018007. [https://doi.org/10.1061/\(ASCE\)NH.1527-6996.0000302](https://doi.org/10.1061/(ASCE)NH.1527-6996.0000302)
- Song L, Li JH, Zhou T, Fredlund DG (2017) Experimental study on unsaturated hydraulic properties of vegetated soil. *Ecol Eng* 103:207–216. <https://doi.org/10.1016/j.ecoleng.2017.04.013>
- Song L, Li J, Gary A, Mei G (2018) Experimental study on water exchange between crack and clay matrix. *Geomech Eng* 14:283–291. <https://doi.org/10.12989/gae.2018.14.3.283>
- Steger S, Brenning A, Bell R, Glade T (2017) The influence of systematically incomplete shallow landslide inventories on statistical susceptibility models and suggestions for improvements. *Landslides* 14:1767–1781. <https://doi.org/10.1007/s10346-017-0820-0>
- Tarolli P, Tarboton DG (2006) A new method for determination of most likely initiation points and the evaluation of Digital Terrain Model scale in terrain stability mapping. *Hydrol Earth Syst Sci* 10:663–677
- Wang HJ, Xiao T, Li XY, Zhang LL, Zhang LM (2019) A novel physically-based model for updating landslide susceptibility. *Eng Geol* 251:71–80. <https://doi.org/10.1016/j.enggeo.2019.02.004>
- Wu C-H, Chen S-C (2009) Determining landslide susceptibility in Central Taiwan from rainfall and six site factors using the analytical hierarchy process method. *Geomorphology* 112:190–204. <https://doi.org/10.1016/j.geomorph.2009.06.002>
- Zhang J, Zhang LM, Tang WH (2011) New methods for system reliability analysis of soil slopes. *Can Geotech J* 48:1138–1148. <https://doi.org/10.1139/t11-009>
- Zhang LL, Zhang J, Zhang LM, Tang WH (2011) Stability analysis of rainfall-induced slope failure: a review. *Proc Inst Civil Eng Geotech Eng* 164:299–316. <https://doi.org/10.1680/geng.2011.164.5.299>
- Zhang LL, Fredlund DG, Fredlund MD, Wilson GW (2014) Modeling the unsaturated soil zone in slope stability analysis. *Can Geotech J* 51:1384–1398. <https://doi.org/10.1139/cgj-2013-0394>
- Zhang YG, Tang J, Liao RP, Zhang MF, Zhang Y, Wang XM, Su ZY (2020) Application of an enhanced BP neural network model with water cycle algorithm on landslide prediction[J]. *Stoch Env Res Risk Assess*. <https://doi.org/10.1007/s00477-020-01920-y>
- Zhao Y, Wang R, Jiang Y, Liu H, Wei Z (2019) GIS-based logistic regression for rainfall-induced landslide susceptibility mapping under different grid sizes in Yueqing. *Southeastern China Eng Geol* 259:105147. <https://doi.org/10.1016/j.enggeo.2019.105147>
- Zhu H, Zhang L (2019) Root-soil-water hydrological interaction and its impact on slope stability. *Georisk: Assess Manag Risk Eng Syst Geohazards* 13:349–359

**Publisher's Note** Springer Nature remains neutral with regard to jurisdictional claims in published maps and institutional affiliations.